The helix-fan transition in the square planar model

1993 J. Phys.: Condens. Matter 5 7121

(http://iopscience.iop.org/0953-8984/5/38/008)

J. Phys.: Condens. Matter 5 (1993) 7121–7130. Printed in the UK

The helix–fan transition in the square planar model

E Rastelli, S Sedazzari and A Tassi
Dipartimento di Fisica dell'Universita, 43100 Parma, Italy

Received 6 April 1993, in final form 28 June 1993

Abstract. Non-collinear spin configurations in an external magnetic field are widely studied but many features await a satisfactory understanding. The phase diagram for a three-sublattice configuration is known when the zero-field helix is supported either by lattice frustration or by exchange competition, but generic helix configurations need further effort. Here we consider the classical square planar model with competing exchange interaction up to third neighbours. In particular, we are interested in the helix configuration with the spin–spin turn angle $Q = \frac{2}{5}\pi$ for which we give a low-temperature expansion of the free energy within the harmonic approximation and Monte Carlo simulation. Our results support the existence of a first-order helix–fan transition at finite temperatures for a field of about half the saturation field, in agreement with a previous guess based on zero-temperature energy calculation.

1. Introduction

The behaviour of interacting spin models with continuous symmetry in an external magnetic field is a topic of current interest [1]. A detailed analysis of the triangular planar antiferromagnetic (TPA) and classical triangular Heisenberg antiferromagnet (TCHA) based on analytic low-temperature expansion of the free energy [2] and on Monte Carlo simulation [3] has elucidated the complicated phase diagram in the H–T plane consisting of a distorted helix configuration, an 'up–up–down' phase and an asymmetric fan phase in addition to the paramagnetic saturated configuration. Analytic calculations based on the harmonic approximation [4] suggest that the phase diagram of the triangular quantum Heisenberg antiferromagnet (TQHA) is similar to that of the corresponding classical model (TCHA) even though at zero temperature the stabilization of the 'up–up–down' phase for a finite range of H is assured by quantum fluctuations. In classical models [5] the 'up–up–down' phase is supported by thermal fluctuations. It is interesting that the TQHA is suitable for modelling $CsCuCl_3$, an ABX_3 hexagonal compound, where A is an alkali element, B is a transition-metal ion and X can be Cl, Br or I. Indeed the intrachain ferromagnetic spin–spin interaction does not cause qualitative peculiarities in the uniform mode energy so that the magnetic resonance data were satisfactorily fitted [6]. We note that the phenomenology of the TPA and related models proves that the expectation based on the extrapolation to intermediate fields of the low- and high-field expansions of the zero temperature energy [7] is not always verified. A first-order 'distorted helix–fan' phase transition is indeed suggested as the generic scenario of helices in an external magnetic field [7] whereas in the TPA the 'up–up–down' phase intervenes in between the helix and the fan phase. A zero-temperature calculation of the energy and of the static structure factor, for both linear and square spin lattices [8, 9] with a magnetic order commensurate with the underlying lattice, leads to a first-order distorted helix–fan phase transition only if the spin–spin turn angle Q is less than $\frac{1}{2}\pi$. Here we consider the 3N model [9, 10] (a square spin lattice with exchange interactions up to third neighbours) at finite temperature for exchange competition inducing

0953-8984/93/387121+10$07.50

a regular helix with $Q = \frac{2}{5}\pi$ at zero temperature and zero field. Assuming that the commensuration with the underlying lattice survives the switching of the magnetic field, we have expanded the free energy near the classical minimum-energy configuration by keeping bilinear contributions and we have found that the low-temperature low-field configuration corresponds to a distorted helix with a spin over five parallel to the field. Note that the pinning of a generic commensurate helix in the low-temperature low-field limit is proven on the basis of an exact expansion [1] where singular delta-like commensuration contributions occur in a natural way. For the particular helix with $Q = \frac{2}{5}\pi$ we obtain in section 2, the elementary excitation spectrum which is characterized by finite-energy uniform modes when the magnetic field is not zero. The zero-temperature energy is characterized by a window of reduced magnetic field $h_1 < h < h_2$ in which two minima are simultaneously present, one corresponding to a distorted helix, and the other to a symmetric fan. Both configurations have one spin over five parallel to the magnetic field. No other minima exist for configurations with five spins per magnetic cell. We have obtained the magnetization as a function of the magnetic field and temperature. The first-order helix–fan phase transition occurs at a critical value h_c of the field which decreases with increasing temperature. We find that the elementary excitation energy corresponding to the fan configuration becomes negative at a certain wavevector, for $h < h_1^*$ where $h_1^* > h_1$. The same occurs for the elementary excitation energy of the distorted helix configuration for $h > h_2^*$ where $h_2^* < h_2$, so that we cannot explore the complete range $h_1 < h < h_2$ where the coexisting minima of the energy are present. Possibly these instabilities are related to the appearance of excitations suitable for driving continuously the fan into the helix for $h = h_1^*$ and the helix into the fan for $h = h_2^*$, moving throughout a wider parameter space than the space that we are considering. However, our results, which work for $h_1^* < h < h_2^*$, give a clear indication that the coexistence curve of the distorted helix and fan configuration is asymmetric with respect to a 'critical point' beyond which the distorted helix changes continuously into the saturated configuration as the field increases at a fixed temperature. We have substantiated this scenario by Monte Carlo simulations (section 3), which show that the change in the configuration becomes continuous for a sufficiently high temperature. Also the static structure factor shows that a substantial weight transfer from the satellite peak at $q = Q = (\frac{2}{5}\pi, 0)$ to the central peak occurs in a magnetic field range which suffers from a dramatic shrinkage for a sufficiently low temperature. Even though we cannot push the Monte Carlo simulation to the lowest temperature to cover the region of temperatures (and fields) where the harmonic approximation is reliable, low-temperature expansion and Monte Carlo simulation give complementary and consistent information about the behaviour of a helix configuration with a spin–spin turn angle less than $\frac{1}{2}\pi$. We confirm the guess [9] based on zero-temperature calculation concerning the dramatic difference between the response to the magnetic field for $Q < \frac{1}{2}\pi$ and that for $Q \geqslant \frac{1}{2}\pi$.

2. Low-temperature thermodynamics in the harmonic approximation

The Hamiltonian that we consider is

$$\mathcal{H} = -J_1 \sum_{i,\delta_1} \boldsymbol{S}_i \cdot \boldsymbol{S}_{i+\delta_1} - J_2 \sum_{i,\delta_2} \boldsymbol{S}_i \cdot \boldsymbol{S}_{i+\delta_2} - J_3 \sum_{i,\delta_3} \boldsymbol{S}_i \cdot \boldsymbol{S}_{i+\delta_3} - \mu \sum_i \boldsymbol{H} \cdot \boldsymbol{S}_i \qquad (2.1)$$

where i labels the sites of a square lattice, δ_α ($\alpha = 1, 2, 3$) is a vector joining the site i with its neighbours of the αth shell and $\boldsymbol{S}_i$ is a two-component classical vector. For simplicity we choose $S = 1$. The zero-field zero-temperature phase diagram of this model consists of four phases characterized by $Q = (0, 0)$ (F), $Q = (\pi, 0)$ (AF), $Q = (\cos^{-1}[(1 - 2j_2)/4j_3], 0)$

(H_1) and $Q = (\cos^{-1}[-1/(2j_2 + 4j_3)], \cos^{-1}[-1/(2j_2 + 4j_3)])$ (H_2). We focus on the line $j_2 = -\frac{1}{2}[j_3(\sqrt{5} - 1) + 1$ for $-1/(3 + \sqrt{5}) < j_3 < 0$, where $Q = (\frac{2}{5}\pi, 0)$ at zero temperature. We define $j_2 = J_2/J_1$, $j_3 = J_3/J_1$. An exact low-temperature low-field free-energy expansion for a generic helix proves that non analytic contributions lock commensurate configurations when an external in-plane magnetic field is applied [1]. For this reason we consider a magnetic cell of five spins. The corresponding reduced energy is

$$\begin{aligned} e_0 = E_0/2J_1N = -\tfrac{1}{5}\{&5(1 + j_3) + (1 + 2j_2)[\cos(\phi_1 - \phi_2) + \cos(\phi_2 - \phi_3) \\ &+ \cos(\phi_3 - \phi_4) + \cos(\phi_4 - \phi_5) + \cos(\phi_5 - \phi_1)] + j_3[\cos(\phi_1 - \phi_3) \\ &+ \cos(\phi_2 - \phi_4) + \cos(\phi_3 - \phi_5) + \cos(\phi_4 - \phi_1) + \cos(\phi_5 - \phi_2)] \\ &+ h(\cos\ \phi_1 + \cos\ \phi_2 + \cos\ \phi_3 + \cos\ \phi_4 + \cos\ \phi_5)\} \end{aligned} \tag{2.2}$$

where $h = \mu H/2J_1$, and ϕ_i (i=1,...,5) is the angle between the ith spin in the unit cell and the external magnetic field, as shown in figure 1(a). The minimum-energy conditions are

$$\begin{aligned} (1 + 2j_2)[\sin(\phi_i - \phi_{i+1}) + \sin(\phi_i - \phi_{i-1})] + j_3[\sin(\phi_i - \phi_{i+2}) + \sin(\phi_i - \phi_{i-2})] \\ + h\ \sin\ \phi_i = 0 \end{aligned} \tag{2.3}$$

with $i = 1, 2, ..., 5$. One has to replace $i \pm n$ by $i \pm n \mp 5$ when $i + n > 5$ or $i - n < 1$. It can be proven that equation (2.3) is satisfied by the configuration with a spin parallel to the field ($\phi_1 = 0$) and the remaining four spins forming angles ϕ_2, ϕ_3, $-\phi_3$ and $-\phi_2$ with the field. This is indeed the zero-temperature minimum-energy configuration with ϕ_2 and ϕ_3 given by the numerical solution of the minimum-energy conditions (2.3) that reduce to

$$\sin\ \phi_2\ [(\sqrt{5} - 2)\ \cos\ \phi_3 - 2\ \cos\ \phi_2 + \sqrt{5} - 1 - h/j_3] = \sqrt{5}\ \cos\ \phi_2\ \sin\ \phi_3 \tag{2.4a}$$

$$\sin\ \phi_3\ [(\sqrt{5} - 2)\ \cos\ \phi_2 + 2(\sqrt{5} - 1)\ \cos\ \phi_3 - 1 - h/j_3] = \sqrt{5}\ \cos\ \phi_3\ \sin\ \phi_2. \tag{2.4b}$$

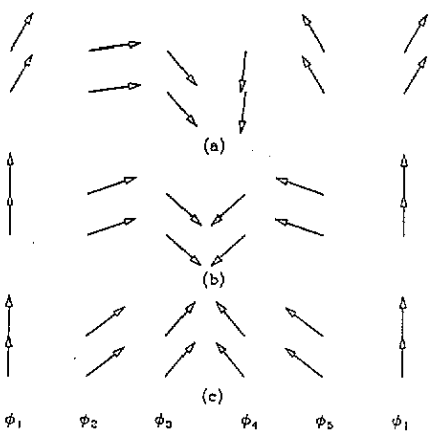

Figure 1. (a) Unit magnetic cell with five spins; (b) distorted helix for $h = 0.05$; (c) symmetric fan for $h = 0.15$.

Figure 1(b) and 1(c) show typical spin configurations for the distorted helix and the symmetric fan, respectively. For vanishing h we give the analytic expressions of ϕ_2 and ϕ_3 that correspond to a weakly distorted helix:

$$\phi_2 = \tfrac{2}{5}\pi - 0.275\,28(h/|j_3|) \tag{2.5a}$$

$$\phi_3 = \tfrac{4}{5}\pi - 0.170\,13(h/|j_3|). \tag{2.5b}$$

In the neighbourhood of the saturation field $h_s = \frac{5}{2}|j_3|(3-\sqrt{5})$, where the fan configuration is stable, one has

$$\phi_2 = 0.905\,79\big[(h_s - h)/|j_3|\big]^{1/2} \tag{2.6a}$$

$$\phi_3 = 0.559\,81\big[(h_s - h)/|j_3|\big]^{1/2}. \tag{2.6b}$$

We have verified by careful numerical sampling of the function (2.2) that no other minima exist except those given by (2.4) even if the hypothesis of a symmetric arrangement of the spins with respect to the field is abandoned. The solution of these equations corresponds to a distorted helix ($h < h_1 = 0.753\,27|j_3|$) and to a symmetric fan configuration $h > h_2 = 1.024\,73|j_3|$). There is a coexistence region corresponding to $h_1 < h < h_2$. The value of h where the zero temperature energies of the two configurations are equal is $h_c = 0.875\,72|j_3|$. As for numerical calculations, we focus on $j_3 = -\frac{1}{8}$ for which $h_1 = 0.094\,16$, $h_2 = 0.128\,09$, and $h_c = 0.109\,46$. At finite temperatures we allow fluctuations around the minimum-energy configuration and we neglect Hamiltonian contributions containing more than two fluctuations, so obtaining

$$\mathcal{H} = E_0 + \mathcal{H}_2 \tag{2.7}$$

where

$$\mathcal{H}_2 = 2J_1 \sum_{s,s'=1}^{5} \sum_{q} \psi_{-q}^{(s)} A_q^{ss'} \psi_q^{(s')} \tag{2.8}$$

where

$$\psi_q^{(s)} = \frac{1}{\sqrt{\frac{1}{5}N}} \sum_i \psi_i^{(s)} \exp\big(-iq \cdot r_i\big) \qquad s = 1, 2, ..., 5 \tag{2.9}$$

is the Fourier transform of $\psi_i^{(s)}$ which is the small deviation that the sth spin in the ith magnetic cell makes with respect to the minimum energy configuration. The elements $A_q^{ss'}$ of the Hermitian matrix $\mathbf{A}_q$ are given in the appendix. The reduced free energy $f = F/2J_1N$ in the harmonic approximation is

$$f = e_0 + \tfrac{1}{2}t \ln\left(\frac{4\pi}{t}\right) + \frac{t}{2}\frac{1}{(\pi)^2}\int_0^{\pi/5} dq_x \int_0^{\pi} dq_y \ln(\det \mathbf{A}_q) \tag{2.10}$$

where $t = k_B T/2J_1$. We stress that the anharmonic contributions that we have neglected are of higher order in temperature so that we expect that the harmonic approximation is reliable in the low temperature limit. In figure 2 we show the free energy of the helix and fan configurations for different temperatures. The zero-temperature energy is double valued in the range $h_1 < h < h_2$, while at finite temperatures the coexistence region is restricted to $h_1^* < h < h_2^*$, where $h_1^* = 0.808\,03|j_3|$ and $h_2^* = 1.022\,41|j_3|$. For $j_3 = -\frac{1}{8}$ one has $h_1^* = 0.101\,00$ and $h_2^* = 0.127\,80$. The fan configuration becomes unstable for $h = h_1^*$ because the determinant of $\mathbf{A}_q$ becomes negative for $h < h_1^*$ owing to the fluctuations in the neighbourhood of $q_x = \frac{1}{5}\pi$, $q_y = 0$. Indeed we have

$$\det \mathbf{A}_q = c_0(h - h^*) + c_1(\tfrac{1}{5}\pi - q_x)^2 + c_2 q_y^2 \tag{2.11}$$

where $c_0 = 7.9794 \times 10^{-5}$, $c_1 = 0.9475 \times 10^{-3}$ and $c_2 = 0.2612 \times 10^{-4}$. An analogous instability occurs for $h > h_2^*$ for the helix configuration at the same wavevector. Note that h_2^* is very close to h_2 so that it is hard to distinguish between them in figure 2. The instabilities at $h = h_1^*$ and $h = h_2^*$ indicate that the fan and helix configurations, which are metastable for $h < h_c(t)$ and for $h > h_c(t)$, respectively, cannot be described by a

magnetic cell of five spins for $h < h_1^*$ and for $h > h_2^*$, so that our calculations based on such a configuration are no longer reliable. It is hard to understand whether the metastable fan (helix) survives in an incommensurate form or whether it fails to exist just for $h = h_1^*$ ($h = h_2^*$). We favour the latter hypothesis because the softening of the fan (helix) elementary excitations for $h = h_1^*$ ($h = h_2^*$) suggests the onset of 'dangerous' excitations in a parameter space wider than that considered. An analogous scenario was found on the F–AF boundary line in the absence of a magnetic field [11]. The dangerous excitations could drive the fan configuration continuously into the helix configuration for $h = h_1^*$ and vice versa for $h = h_2^*$. We expect that h_1^* and h_2^* would be temperature dependent owing to non-linear contributions which are neglected in the harmonic approximation. Moreover, at the critical temperature, $h_1^*(t)$, $h_2^*(t)$, and $h_c(t)$ should meet but this feature cannot be obtained within our approximation. The harmonic approximation leads to the following expectation value of the component along the field of the sth spin of the magnetic cell:

$$\langle \cos(\phi_s + \psi_i^{(s)}) \rangle = \cos\ \phi_s \langle \cos\ \psi_i^{(s)} \rangle \tag{2.12}$$

where

$$\langle \cos\ \psi_i^{(s)} \rangle = \exp\left(-\tfrac{1}{2} t I_{ss}\right) \tag{2.13}$$

with

$$I_{ss} = \frac{5}{(\pi)^2} \int_0^{\pi/5} \mathrm{d}q_x \int_0^{\pi} \mathrm{d}q_y\ \left(\mathbf{A}_q^{-1}\right)_{ss}. \tag{2.14}$$

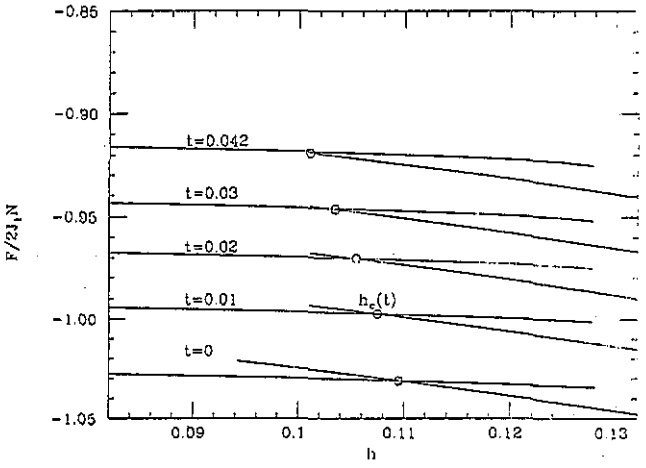

Figure 2. Free energy in the harmonic approximation at the reduced temperatures $t = 0$, 0.01, 0.02, 0.03 and 0.042.

The magnetization can be written

$$m(t) = \tfrac{1}{5}\left[\exp\left(-\tfrac{1}{2} I_{11} t\right) + 2\ \cos\ \phi_2\ \exp\left(-\tfrac{1}{2} I_{22} t\right) + 2\ \cos\ \phi_3\ \exp\left(-\tfrac{1}{2} I_{33} t\right)\right]. \tag{2.15}$$

The integrals (2.14) show non-analytic behaviour for vanishing h owing to the long-wavelength contribution. Indeed we have

$$\left(\mathbf{A}_q^{-1}\right)_{ss} = 2.2767 \times 10^{-4} / \left(0.092\,45 h^5 + 2.57 \times 10^{-3} q_x^2 + 1.36 \times 10^{-3} q_y^2\right) \tag{2.16}$$

which leads to the following result

$$I_{ss} = -0.242\ \ln\ h + \text{regular terms}. \tag{2.17}$$

By putting (2.17) in (2.15) we obtain the low-field behaviour of the magnetization

$$m(t) \simeq 1.157\,78 h^{1+0.121t}. \tag{2.18}$$

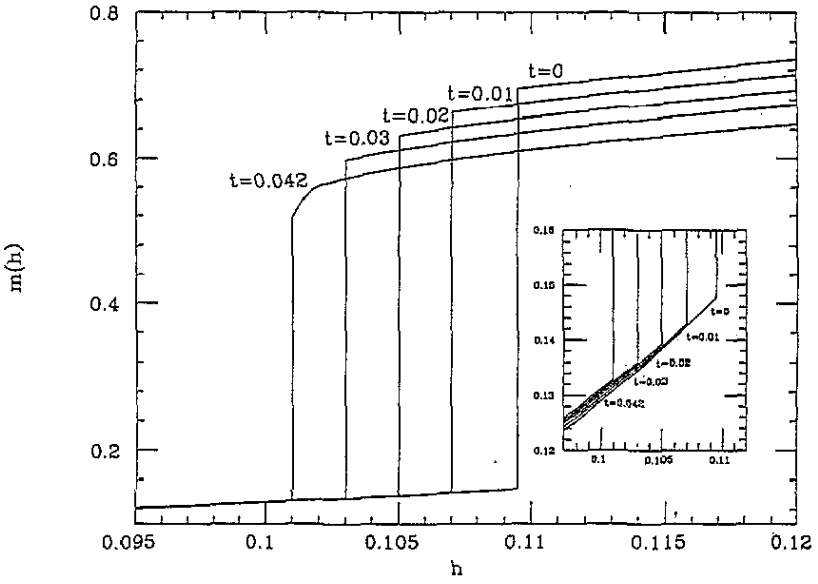

Figure 3. Magnetization per spin in harmonic approximation at the reduced temperatures $t = 0$, 0.01, 0.02, 0.03 and 0.042. The inset clarifies the temperature dependence of the magnetization in the distorted helix configuration.

In figure 3 we show the magnetization for selected values of temperature, where the occurrence of a first-order phase transition is clearly seen. As figure 2 and figure 3 show, the field $h_c(t)$ at which the phase transition occurs decreases with increasing temperature. This temperature dependence can be written as

$$h_c(t) - h_c = \frac{t}{2\pi^2}\int_0^{\pi/5} dq_x \int_0^{\pi} dq_y \frac{\ln(\det \mathbf{A}_q^h) - \ln(\det \mathbf{A}_q^f)}{m^h(0) - m^f(0)}. \tag{2.19}$$

The superscripts h and f mean helix and fan, respectively. All quantities under integration are evaluated at $h = h_c$ in order to avoid spurious contributions. Numerical evaluation of the integral appearing in equation (2.19) gives

$$h_c(t) - h_c = -0.1996t. \tag{2.20}$$

The elementary excitation energies related to the eigenvalues of $\mathbf{A}_q$ which are

$$\hbar\omega_q^{(s)} = 2J_1\lambda_q^{(s)} \qquad s = 1, 2, ..., 5 \tag{2.21}$$

are shown in figure 4 in the (1,0) direction for $h = 0$, $0.32|j_3|$, h_c for the distorted helix. In figure 5 we show the elementary excitation energies for the fan configuration in the (1,0) direction at $h = h_c$, $1.2|j_3|$, h_s.

We have also evaluated $\langle\psi_\parallel\rangle$ and $\langle\psi_\perp\rangle$ the order parameters [5] at zero temperature and low temperatures, respectively, defined by

$$\langle\psi_\parallel\rangle = \tfrac{1}{5}\big[\exp\big(-\tfrac{1}{2}I_{11}t\big) + 2\cos\phi_2\cos\big(\tfrac{2}{5}\pi\big)\exp\big(-\tfrac{1}{2}I_{22}t\big) + 2\cos\phi_3\cos\big(\tfrac{4}{5}\pi\big) \times \exp\big(-\tfrac{1}{2}I_{33}t\big)\big] \tag{2.22}$$

$$\langle\psi_\perp\rangle = \tfrac{2}{5}\big[\sin\phi_2\sin\big(\tfrac{2}{5}\pi\big)\exp\big(-\tfrac{1}{2}I_{22}t\big) + \sin\phi_3\sin\big(\tfrac{4}{5}\pi\big)\exp\big(-\tfrac{1}{2}I_{33}t\big)\big]. \tag{2.23}$$

As one can see in figure 6 the order parameters show clearly the discontinuous helix–fan transition at $h = h_c(t)$. Moreover they vanish for $h = h_s$. Note that the temperature

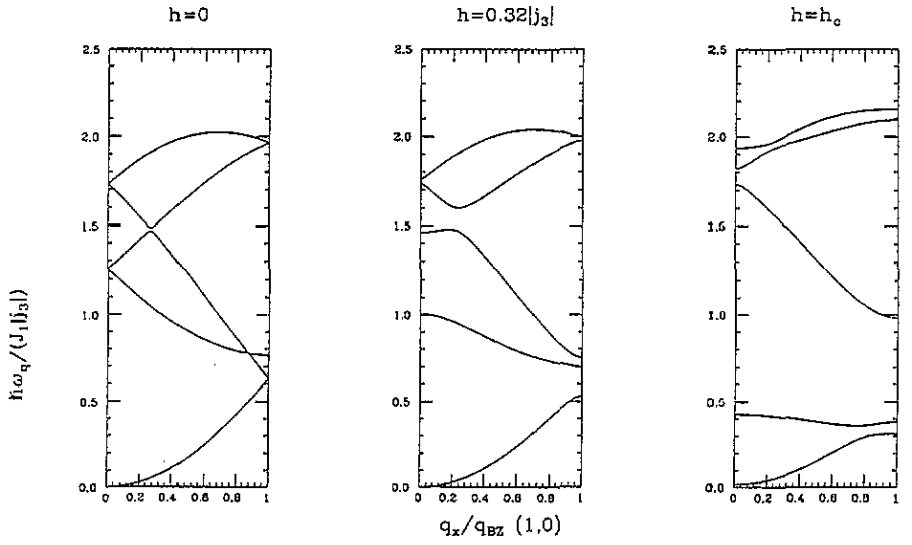

Figure 4. Dispersion curve in the (1,0) direction at $h = 0, 0.32|j_3|, h_c$ for the helix phase.

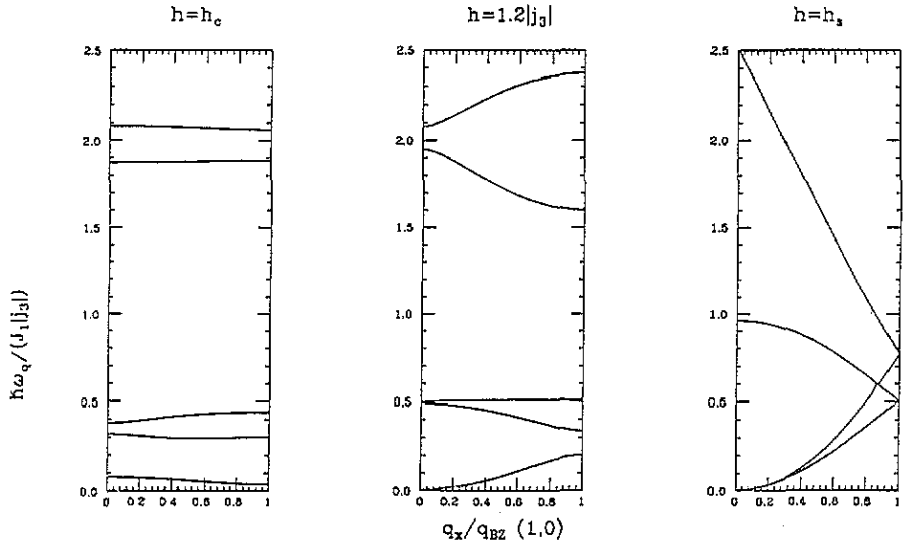

Figure 5. Dispersion curve in the (1,0) direction at $h = h_c, 1.2|j_3|, h_s$ for the fan phase.

dependence of h_s cannot be obtained in the harmonic approximation, because its physical origin is the thermal renormalization of the exchange interactions which is beyond the present approximation.

It is interesting to single out the non-analytic low-field behaviour of the order parameters caused by the singular behaviour of I_{ss} given in equation (2.17). Indeed we have

$$\langle \psi_{\parallel} \rangle \simeq \langle \psi_{\perp} \rangle \simeq (\tfrac{1}{2}) h^{0.121t}. \tag{2.24}$$

Note that equation (2.24) satisfies the Mermin–Wagner theorem [12], giving $\langle \psi_{\parallel} \rangle = \langle \psi_{\perp} \rangle = 0$ for any finite temperature when $h = 0$. However, any finite h assures genuine LRO with a continuous departure from zero but with an infinite slope of the h-dependence.

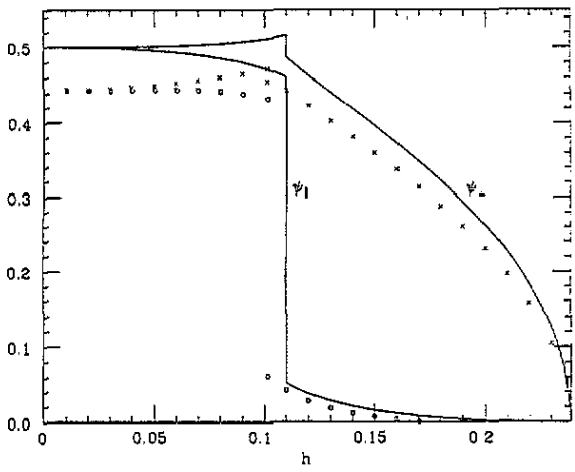

Figure 6. The order parameters $\langle\psi_{\|}\rangle$ (——) and $\langle\psi_{\perp}\rangle$ (——) at $t = 0$ and $\langle\psi_{\|}\rangle$ (○) and $\langle\psi_{\perp}\rangle$ (×) at $t = 0.04$ obtained in the harmonic approximation.

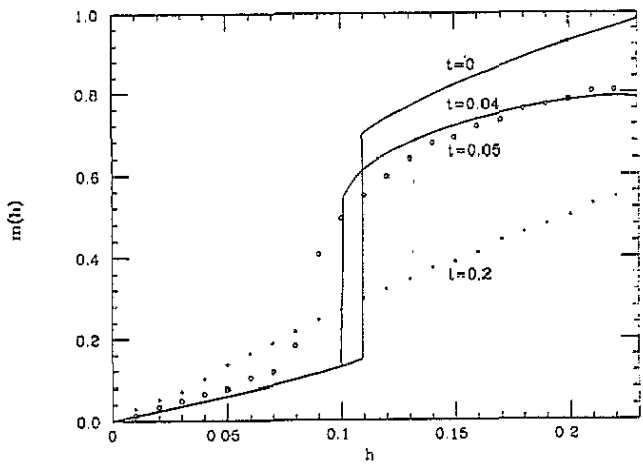

Figure 7. Magnetization versus field as obtained by Monte Carlo simulation in a square lattice of 25×25 spins at $t = 0.05$ (○) and $t = 0.2$ (+): magnetization (——) at $t = 0$ and $t = 0.04$ obtained by the harmonic approximation.

3. Monte Carlo simulation

We have explored the intermediate- and high-temperature range by Monte Carlo simulation on a finite size sample of 25×25 spins with periodic boundary conditions. Our results concerning the magnetization for $t = 0.05$ and $t = 0.2$ are shown in figure 7 by open circles and crosses, respectively. Note that for fields about $h_c(t)$ and $t \simeq 0.05$, a larger number of Monte Carlo steps is required to reach thermalization (200 000 steps against 50 000). Any discontinuous trend disappears completely for $t = 0.2$. The dramatic enhancement in the thermalization time at about $t = 0.05$ suggests that critical phenomena are involved at this temperature. The existence of a first-order phase transition found analytically by harmonic approximation is supported by the results shown in figure 7. The same indication is obtained by the analysis of the static structure factor $S(q_x, q_y)$, i.e. the spatial Fourier transform of the equal-time spin–spin correlation function. $S(q_x, 0)$ at $t = 0.05$ is shown in figure 8 for $h = 0.08$ and $h = 0.09$. Note the substantial transfer of weight from the satellite peak at $q_x = \frac{2}{5}\pi$ to the central peak when the field is slightly changed.

4. Summary and conclusions

In this paper we have analysed the behaviour of the planar model in an external

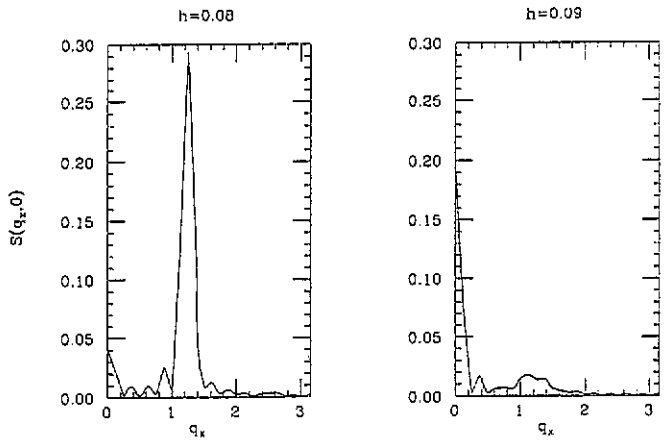

Figure 8. Static structure factor $S(q_x, 0)$ as obtained by Monte Carlo simulation in a square lattice of 25×25 spins at $t = 0.05$ for $h = 0.08$ and $h = 0.09$.

magnetic field for a square lattice where competing spin–spin interaction produces a helix characterized by a turn angle $Q = \frac{2}{5}\pi$ at zero field. Our results are relevant to supporting the hypothesis that a first-order phase transition from the low-field distorted helix to the high-field fan configuration occurs only if $Q < \frac{1}{2}\pi$ in agreement with recent arguments [8,9] given for zero temperature. In section 2 we perform the harmonic approximation and we find that the only commensurate configurations with five spins per magnetic cell are the distorted helix and the fan configuration in addition to the saturated paramagnetic phase. We find the elementary excitation spectrum, the magnetization at a finite temperature and field, and the order parameters. The harmonic approximation supports the existence of a first-order phase transition for a sufficiently low temperature.

In section 3 we perform Monte Carlo simulations on finite-size samples, and the picture that we find at intermediate temperatures is consistent with the analytic results at low temperatures given in section 2. At high temperatures, any signal of a discontinuous change in the spin configuration is completely absent.

The overall scenario of the helix with $Q = \frac{2}{5}\pi$ is very different from that of the helix with $Q = \frac{2}{3}\pi$ extensively studied both analytically and numerically [2,3,5,10]. For $Q = \frac{2}{3}\pi$ any first order helix–fan phase transition is absent and an intermediate phase with two spins parallel and one antiparallel to the field ('up–up–down' phase) intervenes between the low-field and high-field configurations.

Appendix

The elements of the matrix $\mathbf{A}_q$ appearing in equation (2.7) are listed below

$$A_q^{11} = 1 - \cos\ q_y + (1 + 2j_2)\ \cos\ \phi_1 + j_3[1 - \cos(2q_y) + \cos\ \phi_2] + \tfrac{1}{2}h \tag{A1}$$

$$A_q^{22} = 1 - \cos\ q_y + \tfrac{1}{2}(1+2j_2)[\cos(\phi_1 - \phi_2) + \cos\ \phi_1] + j_3\{1 - \cos(2q_y) + \tfrac{1}{2}[\cos(\phi_1 + \phi_2) + \cos(2\phi_1)]\} + \tfrac{1}{2}h\ \cos\ \phi_1 \tag{A2}$$

$$A_q^{33} = 1 - \cos\ q_y + \tfrac{1}{2}(1+2j_2)[\cos(\phi_1 - \phi_2) + \cos(2\phi_2)] + j_3\{1 - \cos(2q_y) + \tfrac{1}{2}[\cos(\phi_1 + \phi_2) + \cos\ \phi_2]\} + \tfrac{1}{2}h\ \cos\ \phi_2 \tag{A3}$$

$$A_q^{44} = A_q^{33} \tag{A4}$$

$$A_q^{55} = A_q^{22} \tag{A5}$$

$$A_q^{12} = -\tfrac{1}{2}\cos\phi_1\,(1 + 2j_2\cos q_y)\,\exp(iq_x) \tag{A6}$$

$$A_q^{13} = -\tfrac{1}{2}j_3\cos\phi_2\,\exp(i2q_x) \tag{A7}$$

$$A_q^{14} = (A_q^{13})^* \tag{A8}$$

$$A_q^{15} = (A_q^{12})^* \tag{A9}$$

$$A_q^{23} = -\tfrac{1}{2}\exp(iq_x)\,\cos(\phi_1 - \phi_2)(1 + 2j_2\cos q_y) \tag{A10}$$

$$A_q^{24} = -\tfrac{1}{2}j_3\cos(\phi_1 + \phi_2)\,\exp(i2q_x) \tag{A11}$$

$$A_q^{25} = -\tfrac{1}{2}j_3\cos(2\phi_1)\,\exp(-i2q_x) \tag{A12}$$

$$A_q^{34} = -\tfrac{1}{2}\exp(iq_x)\,\cos(2\phi_2)(1 + 2j_2\cos q_y) \tag{A13}$$

$$A_q^{35} = A_q^{24} \tag{A14}$$

$$A_q^{45} = -\tfrac{1}{2}\exp(iq_x)\,\cos(\phi_1 - \phi_2)\,(1 + 2j_2\cos q_y). \tag{A15}$$

We recall that $A_q^{ss'} = (A_q^{s's})^*$.

References

[1] see for instance Harris A B, Rastelli E and Tassi A 1991 *Phys. Rev.* B **44** 2624 and references therein

[2] Kawamura H 1984 *J. Phys. Soc. Japan* **53** 2452
Korshunov S E 1986 *J. Phys. C: Solid State Phys.* **19** 5927

[3] Lee D H, Joannopoulos J D, Negele J W and Landau D P 1984 *Phys. Rev. Lett.* **52** 433; 1986 *Phys. Rev.* B **33** 450

[4] Chubukov A V and Golosov D I 1991 *J. Phys.: Condens. Matter* **3** 69

[5] Rastelli E, Tassi A, Pimpinelli A and Sedazzari S 1992 *Phys. Rev.* B **45** 7936

[6] Palme W, Kriegelstein H, Gojkovic G and Lüthi B 1992 *Proceedings of the Transition Metal Conference, (Darmstadt, 1992)*

[7] Nagamiya T 1967 *Solid State Physics* vol 20 (New York: Academic) p 346

[8] Carazza B, Rastelli E and Tassi A 1991 *Z. Phys.* B **84** 301

[9] Rastelli E, Tassi A, Melegari G and Pimpinelli A 1992 *J. Magn. Magn. Mater.* **104** 173

[10] Gallanti C, Rastelli E, Sedazzari S and Tassi A 1993 *J. Appl. Phys.* **73** 5482

[11] Harris A B, Pimpinelli A, Rastelli E and Tassi A 1989 *J. Phys.: Condens. Matter* **1** 3821

[12] Mermin N D and Wagner H 1966 *Phys. Rev. Lett.* **17** 1133